1521-009X/12/4009-1723–1735$25.00
DRUG METABOLISM AND DISPOSITION
Vol. 40, No. 9
45120/3787064

DMD 40:1723–1735, 2012

Excretion and Metabolism of Milnacipran in Humans after Oral Administration of Milnacipran Hydrochloride

Fanying Li, Christina Chin, Julie Wangsa, and John Ho

Forest Research Institute, Farmingdale, New York

Received February 15, 2012; accepted May 31, 2012

ABSTRACT:

The pharmacokinetics, excretion, and metabolism of milnacipran were evaluated after oral administration of a 100-mg dose of [^{14}C]milnacipran hydrochloride to healthy male subjects. The peak plasma concentration of unchanged milnacipran (~240 ng/ml) was attained at 3.5 h and was lower than the peak plasma concentration of radioactivity (~679 ng Eq of milnacipran/ml) observed at 4.3 h, indicating substantial metabolism of milnacipran upon oral administration. Milnacipran has two chiral centers and is a racemic mixture of *cis* isomers: *d*-milnacipran (1*S*, 2*R*) and *l*-milnacipran (1*R*, 2*S*). After oral administration, the radioactivity of almost the entire dose was excreted rapidly in urine (approximately 93% of the dose). Approximately 55% of the dose was excreted in urine as unchanged milnacipran, which contained a slightly higher proportion of *d*-milnacipran (~31% of the dose). In addition to the excretion of milnacipran carbamoyl *O*-glucuronide metabolite in urine (~19% of the dose), predominantly as the *l*-milnacipran carbamoyl *O*-glucuronide metabolite (~17% of the dose), approximately 8% of the dose was excreted in urine as the *N*-desethyl milnacipran metabolite. No additional metabolites of significant quantity were excreted in urine. Similar plasma concentrations of milnacipran and the *l*-milnacipran carbamoyl *O*-glucuronide metabolite were observed after dosing, and the maximum plasma concentration of *l*-milnacipran carbamoyl *O*-glucuronide metabolite at 4 h after dosing was 234 ng Eq of milnacipran/ml. Lower plasma concentrations (<25 ng Eq of milnacipran/ml) of *N*-desethyl milnacipran and *d*-milnacipran carbamoyl *O*-glucuronide metabolites were observed.

Introduction

Milnacipran is a serotonin and norepinephrine reuptake inhibitor, and milnacipran hydrochloride is approved in the United States for management of fibromyalgia (Savella, Forest Laboratories, Inc., 2009) and in other countries for the treatment of depression (Puech et al., 1997). Milnacipran (*Z*-2-aminomethyl-1-phenyl-*N,N*-diethylcyclopropane carboxamide) has two chiral centers and is a racemic mixture of *cis* isomers: *d*-milnacipran (1*S*, 2*R*) and *l*-milnacipran (1*R*, 2*S*). Results from previous pharmacokinetic studies in humans (Puozzo and Leonard, 1996; Puozzo et al., 2002) have shown that milnacipran is rapidly absorbed from the gastrointestinal tract with a median T_{max} of 2 h. The absolute oral bioavailability of milnacipran is high (~85%), and absorption is not affected by food intake. The plasma half-life of milnacipran is approximately 8 h, and approximately 50 to 60% of the dose is excreted in urine as unchanged milnacipran.

The objective of this study was to investigate the metabolism of milnacipran in humans after the oral administration of a 100-mg dose of [^{14}C]milnacipran hydrochloride to healthy male subjects. In addition to determining the pharmacokinetics of milnacipran and radioactivity, the plasma concentrations of milnacipran metabolites were measured. The excretion of radioactivity, milnacipran, and its metabolites were also measured. Furthermore, the chemical structures of milnacipran metabolites were identified.

This work was supported by Forest Research Institute. Medical writing and editorial assistance was also supported by Forest Research Institute.

The clinical phase of this study was conducted by Quintiles Inc. (Overland Park, KS). The authors confirmed that the article is an accurate representation of the study results.

Article, publication date, and citation information can be found at http://dmd.aspetjournals.org.

http://dx.doi.org/10.1124/dmd.112.045120.

Materials and Methods

Chemicals. [^{14}C]Milnacipran hydrochloride with radiochemical purity of 99.0% was synthesized at GE Healthcare (Chalfont St. Giles, Buckinghamshire, UK). Milnacipran, *d*- and *l*-milnacipran, and *N*-desethyl milnacipran standards were obtained from Forest Research Institute (Commack, NY). Glusulase containing 90,000 units/ml β-glucuronidase and 19,000 units/ml sulfatase was purchased from PerkinElmer Life and Analytical Sciences (Waltham, MA). Magnesium chloride hexahydrate, L-α-phosphatidylcholine, D-saccharic acid 1,4-lactone, and UDP-glucuronic acid (UDPGA) trisodium salt were purchased from Sigma-Aldrich (St. Louis, MO). Acetonitrile, deionized water, glacial acetic acid, 12 N hydrochloric acid, methanol, potassium phosphate monobasic, and 10 N sodium hydroxide were purchased from Thermo Fisher Scientific (Waltham MA). Anhydrous sodium acetate and sodium phosphate dibasic were purchased from Mallinckrodt Baker, Inc. (Phillipsburg, NJ). Ammonium acetate and ammonium formate were purchased from Fluka Chemical (St. Louis, MO). Human hepatic microsomes were purchased from BD Gentest (Woburn, MA). Carbon dioxide was purchased from the BOC Group, Inc. (Murray Hill, NJ). All chemicals were analytical grade or better, unless stated otherwise.

Human Mass Balance Study. In this single-center open-label study, six healthy male subjects received a single oral dose of 100 mg of [^{14}C]milnaci-

ABBREVIATIONS: UDPGA, UDP-glucuronic acid; LC, liquid chromatography; MS/MS, tandem mass spectrometry; HPLC, high-performance liquid chromatography; SRM, selected reaction monitoring; LSC, liquid scintillation counting; HRMS, high-resolution mass spectrometry; AUC, area under the curve; dpm, disintegrations per minute.

TABLE 1

Plasma pharmacokinetics of ^{14}C radioactivity and milnacipran after oral administration of a 100-mg dose of [^{14}C]milnacipran hydrochloride to four healthy male subjects

Data are presented as means ± S.D.

Pharmacokinetic Parameters and Units	^{14}C Radioactivity[a]	Milnacipran	Milnacipran (% ^{14}C Radioactivity)
C_{max}, ng/ml	679.0 ± 112.6	239.6 ± 33.2	35.3
AUC_{0-t}, ng · h/ml	6446.3 ± 666.3	2342.6 ± 252.0	36.3
$AUC_{0-\infty}$, ng · h/ml	7325.3 ± 622.1	2766.5 ± 413.2	37.8
T_{max}, h	4.3 ± 0.5	3.5 ± 1.0	
$t_{1/2}$, h	7.7 ± 1.0	8.9 ± 3.2	

[a] Units for C_{max} are nanogram equivalents of milnacipran times milliliter; units for AUC_{0-t} and $AUC_{0-\infty}$ are nanogram equivalents of milnacipran times hour per milliliter.

pran hydrochloride solution (5 ml of 20 mg/ml) at 8:00 AM after breakfast at 7:30 AM. The specific activity of the dose was 1 μCi/mg milnacipran hydrochloride. After oral administration of [^{14}C]milnacipran hydrochloride to pigmented mice, rats, and monkeys, radioactivity (milnacipran and/or metabolites) was distributed into the tissues of the animals (data on file, company study reports). Although radioactivity was observed in the uveal tract (a melanin-rich tissue) of the pigmented mice and monkeys, the elimination of radioactivity from the uveal tract of the animals' eyes indicated that a metabolism study could be safely conducted in humans using a 100 μCi dose of [^{14}C]milnacipran hydrochloride.

Blood samples were collected in prechilled tubes containing tripotassium EDTA before dosing and at 0.5, 1, 1.5, 2, 2.5, 3, 4, 5, 6, 8, 10, 12, 18, 24, 48, 72, 96, and 120 h postdose. Within 30 min from time of collection, plasma was harvested after the centrifugation of blood samples at ≥2500*g* for 10 min at 4°C. Urine samples were collected and pooled from −2 to 0 h predose and at 0 to 4, 4 to 8, 8 to 12, 12 to 24, 24 to 48, 48 to 72, 72 to 96, and 96 to 120 h postdose. Feces samples were collected from day −1 to day 6 and were pooled into 24-h samples (0–24, 24–48, 48–72, 72–96, and 96–120 h); a predose feces sample was collected and pooled from −12 to 0 h. After collection, all samples (plasma, urine, and feces) were kept frozen at −80°C until analysis. Subjects were released from the study on day 6 after one of the following criteria had been met: 1) two consecutive urine and feces samples contained <3 times the radioactivity of the background or 2) the radioactivity excreted in a day was <1% of the radioactivity in the dose (expressed simply as percentage of the dose).

After oral administration of [^{14}C]milnacipran hydrochloride, two of the six subjects vomited (data on file, company study report). Pharmacokinetic analysis and the evaluation of mass balance and metabolite profile were conducted on samples collected from the remaining four subjects. However, the metabolite profile in feces was not evaluated because <4% of the dose was excreted in feces.

All subjects completed an informed consent form at prescreening for the study. The study was approved by the Heartland Institutional Review Board and conducted at Quintiles Inc. (Kansas City, MO) in accordance with the International Conference on Harmonisation Guidance on General Considerations for Clinical Trials, Nonclinical Safety Studies for the Conduct of Human Clinical Trials for Pharmaceuticals, and Good Clinical Practice: Consolidated Guidance.

Radioactivity Analysis of Plasma, Urine, and Feces Samples. After an aliquot of plasma or urine sample was mixed with 10 ml of Ultima Gold scintillant (PerkinElmer Life and Analytical Sciences), the radioactivity concentration of the sample was measured for 5 min using a Packard Tri-Carb 3100 TR Liquid Scintillation Analyzer (PerkinElmer Life and Analytical Sciences). The radioactivity concentration was converted to milnacipran concentration (nanogram equivalents of milnacipran per milliliter) based on the specific activity of the dose. Feces samples were homogenized in water using a Tekmar Lab Blender (Teledyne Technologies, Inc., Mason, OH). Weighed aliquots, in triplicate, of each homogenized feces sample (simply expressed as feces samples unless stated otherwise) were combusted in a Packard Sample Oxidizer model 307 (PerkinElmer Life and Analytical Sciences). After the addition of Carbo-Sorb E and Permafluor E scintillant (10 ml each; PerkinElmer Life and Analytical Sciences) to the combustion products of the feces samples, the radioactivity concentration of the feces samples was measured over a 5-min period using the Packard Tri-Carb 3100 TR Liquid Scintillation Analyzer and then converted to milnacipran concentration (nanogram equivalents of milnacipran per gram) on the basis of the specific activity of the dose. The oxidizer recovery was determined by combustion of ^{14}C standards in an identical manner. The amounts of radioactivity (expressed in milnacipran) excreted in urine and feces were determined and used to evaluate mass balance of the dose.

Analysis of Unchanged Milnacipran. The plasma concentration of unchanged milnacipran was determined by a validated liquid chromatography-tandem mass spectrometry (LC-MS/MS) method. After the supernatant of the plasma sample (or standard) was mixed with the [$^2H_{10}$]milnacipran internal standard and mobile phase [120 mM formic acid-water-methanol (200:1200:600, v/v/v)], the components in the mixture were separated using a Symmetry C8 column (100 × 2.1 mm, 3.5 μm particle size; Waters, Milford, MA) with an isocratic elution of mobile phase at 0.25 ml/min. Temperatures of the autosampler and the high-performance liquid chromatography (HPLC) column were kept at 15 and 30°C, respectively. The LC system (Agilent 1100; Agilent Technologies, Waldbronn, Germany) was interfaced to an API 3000 triple quadruple mass spectrometer (AB Sciex, Toronto, ON, Canada). Electrospray ionization of the mass spectrometer was set to positive ion multiple reaction monitoring mode (precursor ion → product ion) as follows: milnacipran, *m/z* 247.1 → 230.2; internal standard, *m/z* 257.1 → 240.2. Protonated molecular ions of milnacipran and the internal standard were the precursor ions for this analysis. The ratio of milnacipran product ion peak area to that of its internal standard (peak area ratio of milnacipran) was the response used for quantification. The method was linear over a milnacipran concentration range of 5 to 2000 ng/ml with a lower limit of quantification of 5 ng/ml in 25 μl of human plasma. Quality control samples containing 15, 500, and 1600 ng/ml milnacipran were also analyzed. Unless stated otherwise, the concentration of milnacipran determined by LC-MS/MS analysis is expressed as the amount of milnacipran free base per unit volume.

Metabolite Profile Analysis. To acquire sufficient volumes for qualitative and quantitative analyses of the plasma metabolites, samples from the four subjects who did not vomit were used to prepare 14 plasma pools according to time of collection (0.5, 1, 1.5, 2, 2.5, 3, 4, 5, 6, 8, 10, 12, 18, and 24 h postdose). One milliliter of plasma from each subject was used to prepare the pool. Unless stated otherwise, the analysis of the plasma pools was simply described as the analysis of the plasma. Urine samples (0–4, 4–8, 8–12, 12–24, 24–48, 48–72, and 72–96 h postdose) from the four subjects were also analyzed to establish the metabolite profile. For the chiral LC-selected reaction monitoring (LC-SRM) analysis of milnacipran enantiomers, a 0 to 96 h urine pool was prepared for each subject by mixing 0.1% (by volume) of each urine sample of the subject collected in 96 h after dosing.

Sample preparation. After 3 ml of acetonitrile was mixed with 1 ml of plasma sample by vortex for approximately 30 s, the mixture was kept at room temperature for approximately 10 min and then centrifuged at 14,000 rpm for 15 min. The supernatant was transferred to a clean test tube and evaporated to dryness in a TurboVap evaporator under a gentle flow of nitrogen. The sample residue was reconstituted in 400 μl of 1 M ammonium acetate (pH 5)-water-

TABLE 2

Cumulative excretion after oral administration of a 100-mg dose of [^{14}C]milnacipran hydrochloride to four healthy male subjects

Data are presented as means ± S.D.

Period	Excretion		
	Urine	Feces	Total
	% dose		
0–4 h	24.8 ± 1.9	N.A.	24.8 ± 1.9
0–8 h	48.5 ± 5.1	N.A.	48.5 ± 5.1
0–12 h	60.8 ± 6.7	N.A.	60.8 ± 6.7
0–24 h	79.4 ± 4.6	0.407 ± 0.2	79.6 ± 4.8
0–48 h	89.3 ± 2.8	2.83 ± 0.9	92.2 ± 3.2
0–72 h	92.1 ± 2.2	3.27 ± 1.5	95.4 ± 2.0
0–96 h	92.8 ± 1.7	3.62 ± 1.1	96.5 ± 1.1
0–120 h	93.1 ± 1.5	3.65 ± 1.1	96.8 ± 0.7
0–144 h	93.3 ± 1.4	3.65 ± 1.1	96.9 ± 0.6

N.A., not applicable because no feces samples were collected.

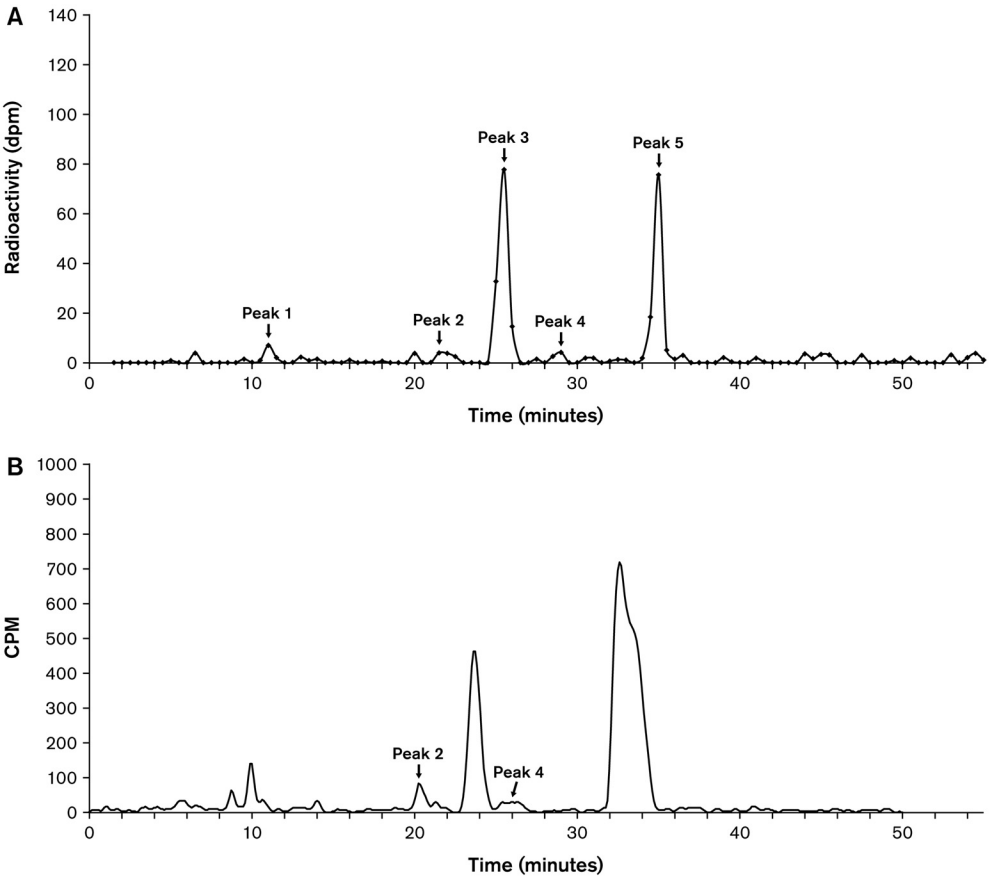

FIG. 1. HPLC chromatogram of the 1.5-h plasma pool (A) and the 4 to 8 h urine sample (B) of subject 3 after oral administration of a 100-mg dose of [^{14}C]milnacipran hydrochloride. *, the retention times of the chromatographic peaks observed in LSC of the HPLC fraction (i.e., procedure for metabolite profile of plasma) was approximately 1 to 2 min longer than those observed in the radioactivity flow detector because of the extra tubing used for collecting the HPLC fractions.

Chromatographic peak	Peak 1 (N-desethyl milnacipran)	Peak 2	Peak 3 (*l*-milnacipran carbamoyl O-glucuronide)	Peak 4 (*d*-milnacipran carbamoyl O-glucuronide)	Peak 5 (milnacipran)
Retention time (min)*	11	22	26	29	35

methanol (2:62.4:35.6, v/v/v) to become the processed plasma sample for analysis. Urine samples were analyzed directly without sample preparation.

Sample analysis. After injection of the urine or processed plasma sample (in 200-μl aliquots) into an Alliance 2690 Separations Module HPLC system (Waters), the components of the sample were separated on a Luna Phenyl-Hexyl column (250 × 4.6 mm, 5 μm particle size; Phenomenex, Torrance, CA) with an Eclipse XDB-C18 guard column (12.5 × 4.6 mm, 5 μm particle size; Agilent Technologies). Temperatures of the autosampler and HPLC column were kept at 10 and 35°C, respectively. The analysis used a gradient elution with flow rate of the mobile phase set at 1 ml/min. Mobile phase A was 1 M ammonium acetate (pH 5)-water-methanol (20:930:50, v/v/v); mobile phase B was 1 M ammonium acetate (pH 5)-water-methanol (20:30:950, v/v/v). The gradient elution was initiated at 34% of mobile phase B for 29 min, ramped to 90% over 11 min, maintained at 90% for 5 min, and returned to the initial condition over 1 min. The column was equilibrated for 9 min at the initial condition between injections. After injection of the processed plasma sample onto the HPLC column, the HPLC eluent was collected in 0.5-min fractions over a period of 54 min, totaling 108 fractions collected from each sample. The radioactivity of each fraction was determined by LSC. The HPLC

TABLE 3

Plasma concentration of milnacipran and its metabolites after oral administration of a 100-mg dose of [^{14}C]milnacipran hydrochloride to four healthy male subjects

Time	Plasma Concentration				
	Peak 1 (*N*-Desethyl Milnacipran)	Peak 2	Peak 3 (*l*-Milnacipran Carbamoyl *O*-Glucuronide)	Peak 4 (*d*-Milnacipran Carbamoyl *O*-Glucuronide)	Peak 5 (Milnacipran)
	ng Eq of milnacipran/ml				
0.5 h	BLOD	BLOD	26.57	BLOD	33.92
1 h	BLOD	BLOD	101.66	BLOD	83.17
1.5 h	BLOD	BLOD	161.30	BLOD	156.73
2 h	BLOD	9.12	190.14	BLOD	178.93
3 h	24.60	12.53	195.72	16.42	208.01
4 h	19.63	BLOD	234.38	17.49	214.21
6 h	23.46	BLOD	140.79	BLOD	186.82
12 h	13.67	BLOD	50.79	BLOD	87.22

BLOD, below limit of detection (i.e., concentration <7.8 ng Eq of milnacipran/ml).

TABLE 4

Metabolite profiles of urine after oral administration of a 100-mg dose of [^{14}C]milnacipran hydrochloride to four healthy male subjects

Data are mean values, calculated on the basis of the number of samples that contained a peak.

Period	Excretion					
	Peak 1	Peak 2	Peak 3	Peak 4	Peak 5	Total
	% dose					
0–4 h	0.92	0.43	6.26	0.55	15.54	
4–8 h	1.35	0.43	5.39	0.64	14.42	
8–12 h	1.26	0.21	2.36	0.37	7.17	
12–24 h	2.06	0.28	2.36	0.58	10.87	
24–48 h	1.36	0.13	0.76	0.28	5.45	
48–72 h	0.73	BLOD	0.19	BLOD	1.47	
72–96 h	0.06	0.07	BLOD	BLOD	0.30	
0–96 h	7.73	1.33	17.23	2.14	54.71	84.26

BLOD, below limit of detection for on-column analysis (approximately 396 cpm/200 μl).

TABLE 5

Urinary excretion of milnacipran enantiomers after oral administration of a 100-mg dose of [^{14}C]milnacipran hydrochloride to four healthy male subjects

Subject	Excretion in 0–96 h Urine Sample		
	l-Milnacipran	*d*-Milnacipran	Milnacipran[a]
		% dose	
1	22.1	33.6	55.7
2	24.4	28.6	53.0
3	23.8	32.4	56.2
4	23.6	30.4	54.0
Mean	23.5	31.2	54.7

[a] Data are from metabolite profiles of urine (Table 4).

eluent from analysis of urine sample was monitored by a radioactivity flow detector with a detection cell that contained solid scintillant (high-pressure lithium glass-packed, 150 μl; IN/US, Tampa, FL). The radioactivity detector was set at 6 s for dwell time and 9 s for time of flight. The HPLC eluent was also monitored by a UV detector. The wavelength of the UV detector was set at 220 nm with a filter of 1 s. The nonradioactive standards were monitored by the UV detector.

Identification of Metabolites. Five chromatographic peaks with measurable radioactivity were found in the plasma and urine metabolite profiles. The metabolites eluted in these peaks were identified using LC-MS/MS, LC-SRM, and LC-high-resolution mass spectrometry (LC-HRMS) methods. Biosynthetic standards were prepared as described below.

Biosynthesis of d- and l-milnacipran carbamoyl O-glucuronide. Based on modifications of a published method (Delbressine et al., 1990), *d*-milnacipran and *l*-milnacipran were incubated with carbon dioxide, human hepatic microsomes, and UDPGA. The resulting *d*- and *l*-milnacipran carbamoyl *O*-glucuronides were purified by HPLC separation and became the biosynthetic standards. The glucuronides were not produced in the absence of carbon dioxide, microsomes, or UDPGA from the incubation. The chemical structures of the biosynthetic standards were characterized by LC-MS/MS, LC-HRMS, and hydrolysis.

LC-MS/MS. Metabolites were identified on an Alliance 2795 Separations Module system (Waters) set at the HPLC conditions described above for the metabolite profile analysis. The LC system was interfaced to a TSQ 7000 triple quadruple mass spectrometer (Thermo Fisher Scientific) with the atmosphere pressure chemical ionization source set at positive ion mode. Metabolites were initially characterized by comparing predose with postdose samples using a full scan (from *m/z* 100 to 650) and profile mode set at 1 s of scan time. Vaporization and capillary temperature were maintained at 500 and 200°C, respectively. Sheath gas (nitrogen) was 60 psi, and corona discharge was 5 μA. The electron multiplier was adjusted to obtain the optimum signals. Structural information of the metabolites was further generated from the product ion spectra of their respective protonated molecular ions.

LC-SRM. To improve sensitivity, identification of plasma metabolites was conducted by SRM of the metabolites based on their product ion spectra. The SRM was set to positive ion mode (precursor ion → product ion) as follows: milnacipran carbamoyl *O*-glucuronide, *m/z* 467 → 230; milnacipran, *m/z* 247 → 230. Protonated molecular ions of milnacipran carbamoyl *O*-glucuronide and milnacipran

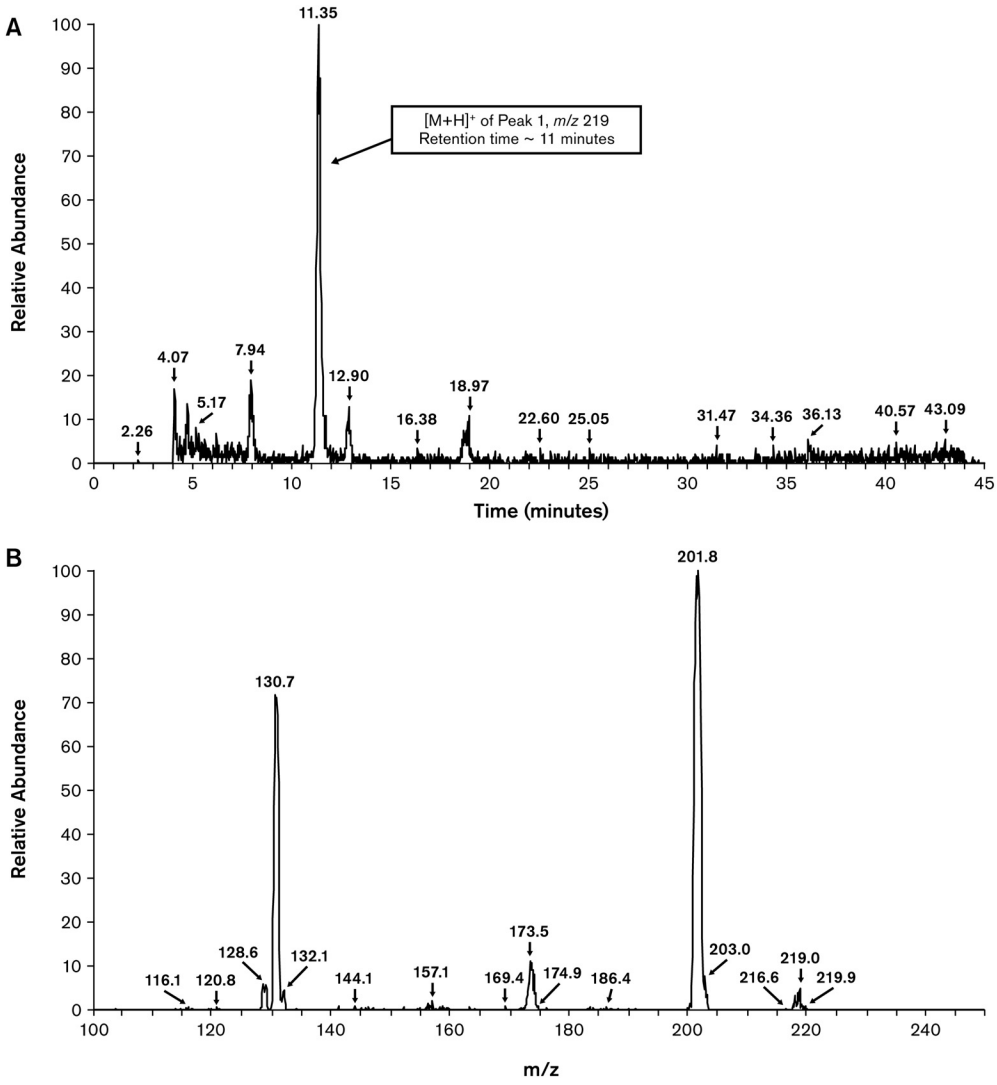

FIG. 2. LC-MS/MS analysis of *N*-desethyl milnacipran metabolite (peak 1, precursor ion = protonated molecular ion, *m/z* 219) in the 0 to 4 h urine sample of subject 1. A, protonated molecular ion of *N*-desethyl milnacipran metabolite. B, product ion spectrum produced by the protonated molecular ion of *N*-desethyl milnacipran metabolite.

were the precursor ions for this analysis. The purpose of measuring milnacipran was to evaluate the potential degradation of the glucuronide to milnacipran in the ionization source of the mass spectrometer (i.e., in-source degradation).

Chiral LC-SRM analysis, conducted on an Alliance 2795 Separations Module (Waters), was used to analyze milnacipran enantiomers in plasma and urine samples. The milnacipran enantiomers were separated on a Chirobiotic V column (150 × 4.6 mm, 5-μm particle size; Advanced Separation Technologies, Inc., Whippany, NJ) with a Chirobiotic V guard column (20 × 4.0 mm; Advanced Separation Technologies, Inc.); the column was eluted with a mobile phase of 1 M ammonium formate-methanol (1:799, v/v) at a flow rate of 1 ml/min. Temperatures of the autosampler and HPLC column were kept at 10 and 20°C, respectively. The SRM setting of milnacipran described above was used for the SRM of milnacipran enantiomers (*m/z* 247 → 230).

LC-HRMS. Structure characterization of metabolites was conducted using an Agilent 1100 series HPLC system (Agilent Technologies) set at the HPLC conditions described above for the metabolite profile analysis. The LC system was interfaced to a QSTAR XL mass spectrometer (AB Sciex). Mobile phases were modified as follows to minimize ion suppression: mobile phase A, 1 M ammonium acetate (pH 5)-water-methanol (5:945:50, v/v/v); mobile phase B, 1 M ammonium acetate (pH 5)-water-methanol (5:45:950, v/v/v). Postcolumn flow was split such that the mobile phase was introduced into the mass spectrometer via an electrospray interface at a rate of 100 μl/min; the remaining flow was diverted as waste. The protonated molecular ion of the metabolite was obtained by time-of-flight scan (*m/z* 100-1000 at an accumulation time of 1 s). The source temperature was maintained at 220°C, and the IonSpray voltage was set at 5500 V. Curtain gas, ion source gas 1, and ion source gas 2 were set at 20, 30, and 10, respectively. Declustering potential 1, declustering potential 2, and focusing potential were set at 30, 15, and 80 V, respectively. Both ion release delay and ion release width were set at 10. The electron multiplier was adjusted to obtain optimum signals.

Hydrolysis of Urine Metabolites. After isolation of peak 3 and peak 4 from the 0 to 4 h urine samples of two subjects, the hydrolytic properties of the metabolites eluted in these peaks were established to support the structures of the milnacipran metabolites.

Isolation. Peak 3 and peak 4 in 1 ml of the 0 to 4 h urine sample collected from subject 1 were isolated after HPLC analysis of the urine sample as five

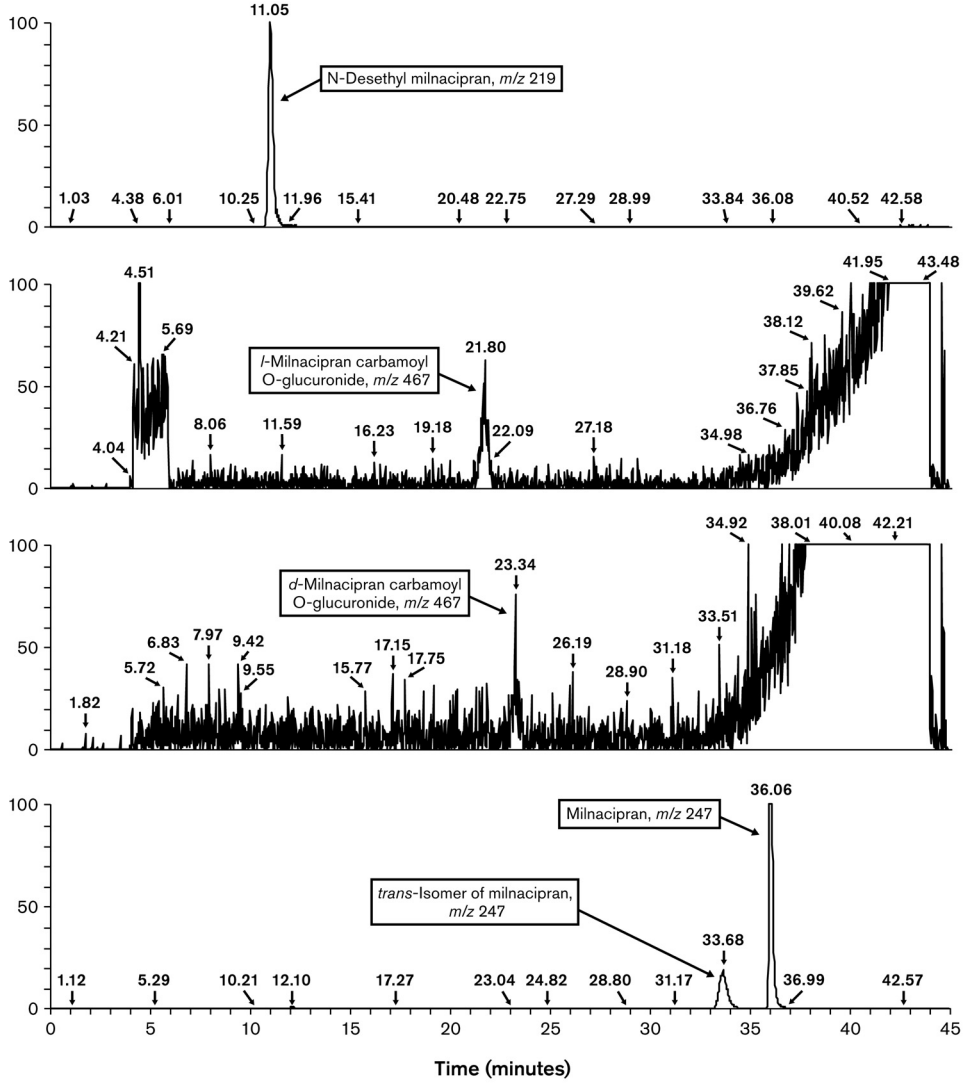

FIG. 3. The LC-MS/MS chromatogram from the analysis of chemically synthesized and biosynthetic standards. The retention times of the chromatographic peaks observed in LC-MS/MS analysis were approximately 1 to 2 min different from those observed in HPLC-radioactivity flow detector analysis because of the different HPLC instrument used. *, chemically synthesized standard; **, biosynthetic standard.

Standard	N-Desethyl milnacipran*	*l*-Milnacipran carbamoyl O-glucuronide**	*d*-Milnacipran carbamoyl O-glucuronide**	*trans*-Isomer of milnacipran*	Milnacipran*
Retention time (min)	11	22	24	34	36
Prolonated molecular ion (*m/z*)	219	467	467	247	247

200-μl aliquots. The HPLC eluent collected between 22 to 25 min was evaporated to dryness in a TurboVap under a gentle flow of nitrogen at 30°C, and the dry residue was then reconstituted by sonification in 250 μl of water and 20 μl of acetonitrile to produce isolated peak 3 of subject 1. The HPLC eluent collected between 26.5 to 28.5 min was also processed to produce the isolated peak 4 of subject 1. Likewise, isolated peak 3 and isolated peak 4 of subject 3 were prepared.

Acid hydrolysis. After the sample (40 μl of isolated peak 3 or peak 4) or biosynthetic standard was mixed with 40 μl of 2 N hydrochloric acid in a glass test tube, the test tube was capped tightly and kept on a heating block at 70°C for 1 h. The samples were then cooled to ambient room temperature and partially neutralized by addition of 24 μl of 2 N sodium hydroxide. These partially neutralized samples were mixed gently by vortex for approximately 30 s, transferred to HPLC vials, and mixed with 24 μl of water and 52 μl of 1 M ammonium acetate (pH 5)-water-methanol (2:62.4:35.6, v/v/v). After centrifugation of the HPLC vials for approximately 5 min, 20 μl of the clear supernatant (hydrolyzed samples) were analyzed by LC-SRM. A nonhydrolyzed control sample [40 μl of sample, 52 μl of 1 M ammonium acetate (pH 5)-water-methanol (2:62.4:35.6, v/v/v), 24 μl of water, and 64 μl of a reagent containing 40 μl of 2 N hydrochloric acid and 24 μl of 2 N sodium hydroxide] was similarly analyzed.

Enzyme hydrolysis. After the sample (40 μl of isolated peak 3 or peak 4) or biosynthetic standard was mixed with 60 μl of 0.2 M sodium acetate buffer at pH 5, 10 μl of water, and 10 μl of Glusulase in a glass test tube, the sample was incubated in a water bath at 37°C for 1 h. The samples were then cooled to ambient room temperature, transferred to HPLC vials, and mixed with 8 μl of water and 52 μl of 1 M ammonium acetate (pH 5)-water-methanol (2:62.4:35.6, v/v/v). After centrifugation of the HPLC vials for approximately 5 min, 20 μl of the clear supernatant (hydrolyzed samples) was analyzed by LC-SRM. A control sample without hydrolysis by Glusulase was analyzed similarly. The inhibition of hydrolysis was evaluated by replacing the water in the enzyme hydrolysis procedure with 100 mg/ml D-saccharic acid 1,4-lactone.

Data Analysis. *Pharmacokinetics and mass balance.* Radioactivity concentrations in plasma, urine, and feces samples were determined at the clinical site using LSC, with combustion as necessary. Raw data (weight/volume and radioactivity concentration) of urine and feces samples collected from each subject were captured in the Debra data capture system (LabLogic Systems, Ltd., Sheffield, UK). Descriptive statistics were used to analyze the excretion of radioactivity in urine and feces (percentage of the dose), as well as the pharmacokinetic parameters of milnacipran and radioactivity.

Pharmacokinetic assessments [area under the plasma concentration-time curve from time 0 up to the last measurable concentration (AUC_{0-t}), AUC from time 0 up to infinity ($AUC_{0-\infty}$), maximum plasma concentration (C_{max}), time to maximum plasma concentration (T_{max}), terminal elimination half-life ($t_{1/2}$), and terminal rate constant (λ_z)] were derived using noncompartmental analysis (Gibaldi and Perrier, 1975) with WinNonlin software (version 4.1 or higher; Pharsight, Mountain View, CA). Plasma concentrations below the limit of quantification were treated as zero for pharmacokinetic calculations with actual sampling times.

The amount of radioactivity excreted in a sample [disintegrations per minute (dpm)] was calculated by multiplying the radioactivity concentration of the sample (disintegrations per minute per milliliter, urine; disintegrations per minute per gram, feces) by the amount of the sample (milliliters, urine; grams, feces). The amount of the radioactivity excreted in a sample (percentage of the dose) was calculated by the following equation:

$$\text{Amount of radioactivity excreted in a sample (\% dose)} = \frac{\text{Amount of radioactivity excreted in a sample (dpm)}}{\text{Amount of radioactivity in the dose (dpm)}} \times 100\%$$

The cumulative excretion in urine and the cumulative excretion in feces for each subject were determined by summing up the excretion at each time interval. Mass balance (the total recovery of radioactivity in the dose) of milnacipran in each subject was the sum of the cumulative excretions in urine and in feces (percentage of the dose) for that subject.

Metabolite profile. The chromatograms of urine samples were recorded and processed by Laura 3 software (version 3.096.119; LabLogic Systems Ltd.) to obtain retention times and maximum signals of the chromatographic peaks (peak area in counts per minute). The background radioactivity was estimated from a blank region of the chromatogram selected arbitrarily after the elution of all chromatographic peaks. The net amount of radioactivity in the chromatographic peak was calculated by subtracting the background radioactivity from the radioactivity in the chromatographic peak. Likewise, the net amount of radioactivity in a HPLC fraction of a plasma sample was calculated by subtracting the background radioactivity of a blank HPLC fraction from the radioactivity in the fraction.

Plasma metabolite profile. The plasma concentration of a metabolite eluted as a chromatographic peak in the metabolite profile of a plasma sample pool was calculated as follows:

$$\text{Plasma concentration of the metabolite in the plasma sample pool (ng Eq of milnacipran/ml)} = \text{Net amount of radioactivity in chromatographic peak of a metabolite (\% total radioactivity in the chromatogram)} \times \text{Concentration of radioactivity in the plasma sample pool (ng Eq of milnacipran/ml)}$$

The concentration of radioactivity in the plasma sample pool (nanogram equivalents of milnacipran per milliliter) was calculated on the basis of the concentration of radioactivity in the plasma samples (data on file, company

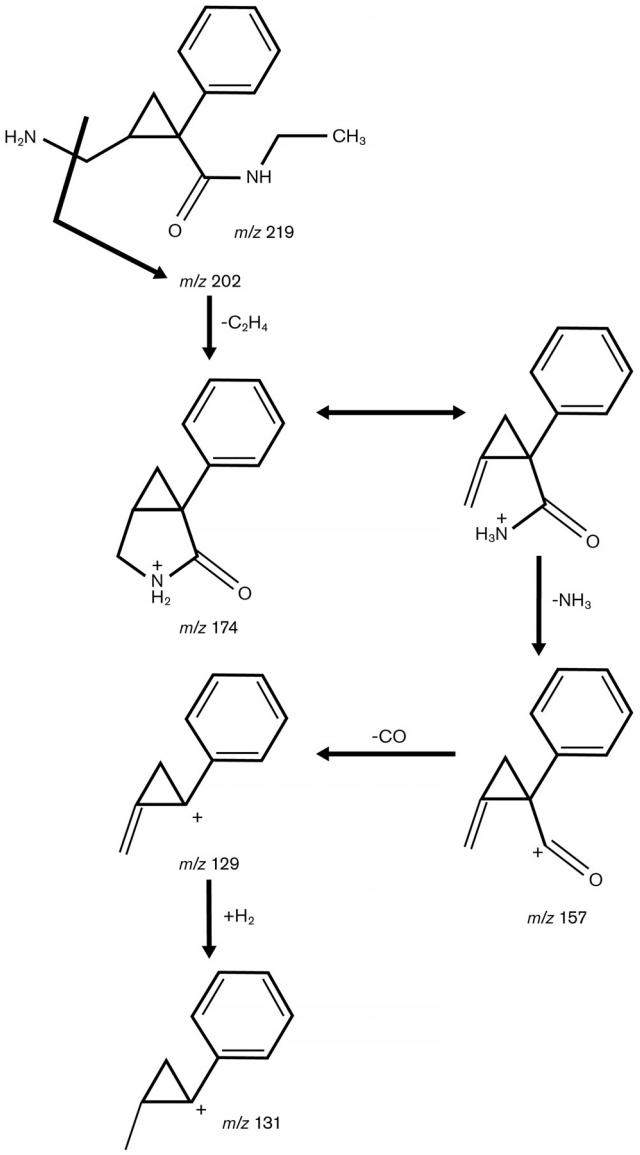

FIG. 4. Proposed fragmentation pattern for the protonated molecular ion of *N*-desethyl milnacipran metabolite, $[M + H]^+$, *m/z* 219.

study report) used for the preparation of the pool. The net amount of radioactivity in the chromatographic peak of the metabolite is expressed as a percentage of total radioactivity found in the chromatogram.

Urine metabolite profile. The excretion (percentageof the dose) of a metabolite eluted as a chromatographic peak in the metabolite profile of a urine sample was calculated as follows:

$$\text{Amount of the metabolite excreted in the urine sample (\% dose)} = \text{Net amount of radioactivity in chromatographic peak of a metabolite (\% total radioactivity in the chromatogram)} \times \text{Amount of radioactivity excreted in the urine sample* (\% dose)}$$

*Data on file, company study report.

The net amount of radioactivity in the chromatographic peak of the metabolite is expressed as a percentage of total radioactivity found in the chromatogram.

Enantiomer composition of milnacipran in urine sample. After chiral LC-SRM analysis of the 0 to 96 h urine pool or urine standard, detector output was recorded and analyzed using Xcalibur software (version 1.1; Thermo Fisher Scientific). Each chromatogram was analyzed to obtain retention times and maximum signals (peak areas) for *d*- and *l*-milnacipran. The amount of milnacipran enantiomer (*d*- or *l*-milnacipran) excreted in the 0 to 96 h urine pool (% of the dose) of an individual subject was calculated as follows:

$$\text{Amount of milnacipran enantiomer excreted in the 0–96 h urine pool (\% dose)} = \text{Proportion of milnacipran enantiomer in the 0–96 h urine pool (\% milnacipran in the urine pool)} \times \text{Amount of milnacipran excreted in the 0–96 h urine pool* (\% dose)}$$

*Data on file, company study report.

The proportion of milnacipran enantiomer (*d*- and *l*-milnacipran) in the 0 to 96 h urine pool (% of milnacipran in the urine pool) was calculated for each subject using the following set of equations:

$$\text{Proportion of } l\text{-milnacipran enantiomer in the 0–96 h urine pool} = \frac{\text{Peak area of } l\text{-milnacipran} \times 100\%}{\text{Peak area of } l\text{-milnacipran} + \left(\text{Peak area of } d\text{-milnacipran} \times \text{Peak area ratio of urine standard}\right)}$$

$$\text{Peak area ratio of urine standard*} = \frac{\text{Peak area of } l\text{-milnacipran in urine standard}}{\text{Peak area of } d\text{-milnacipran in urine standard}}$$

*Urine standard was a racemic mixture with equal amounts of *d*- and *l*-milnacipran.

$$\text{Proportion of } d\text{-milnacipran enantiomer in the 0–96 h urine pool} = 100\% - \text{Proportion of } l\text{-milnacipran enantiomer in the 0–96 h urine pool}$$

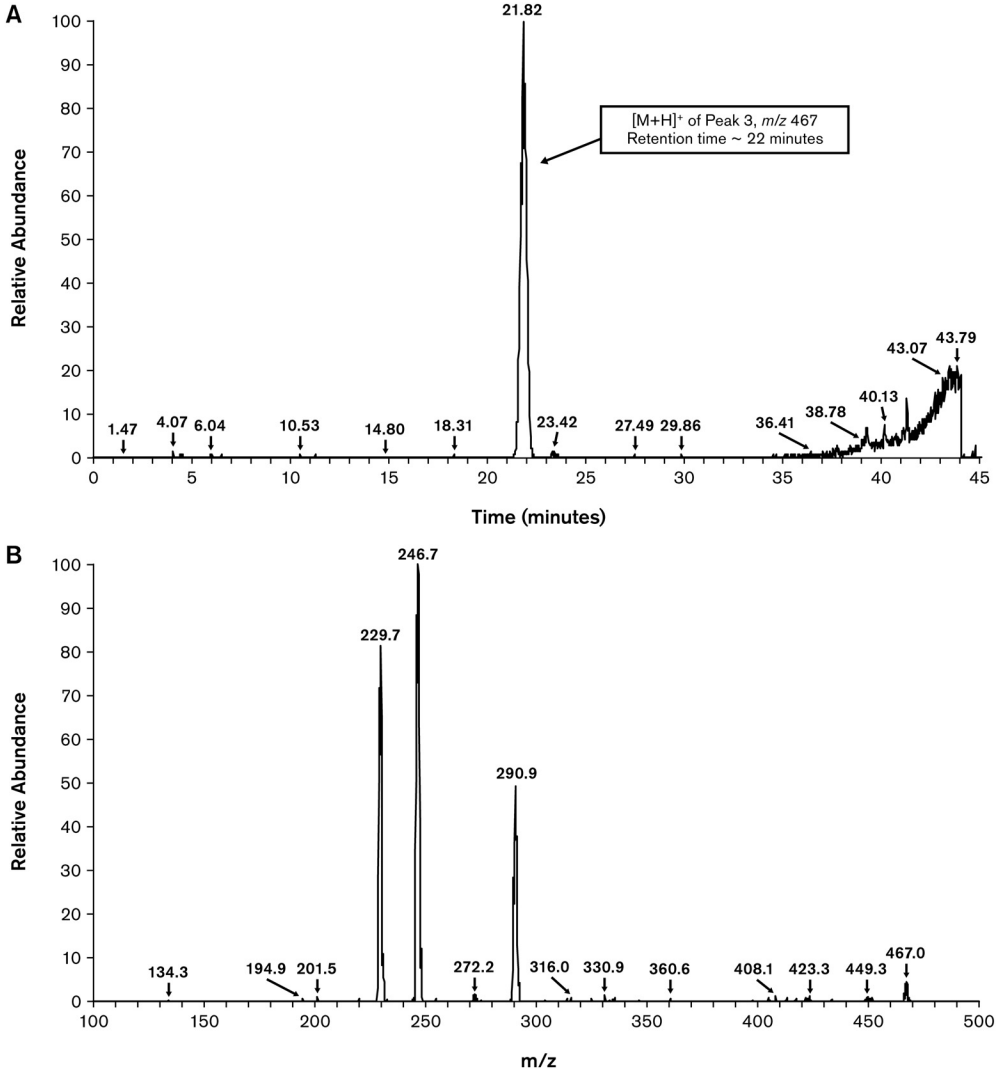

FIG. 5. LC-MS/MS analysis of *l*-milnacipran carbamoyl *O*-glucuronide metabolite (peak 3, precursor ion = protonated molecular ion, *m/z* 467). A, protonated molecular ion of *l*-milnacipran carbamoyl *O*-glucuronide metabolite in the 0 to 4 h urine sample of subject 1. B, product ion spectrum produced by the protonated molecular ion of *l*-milnacipran carbamoyl *O*-glucuronide metabolite in the 0 to 4 h urine sample of subject 3.

Results

Pharmacokinetics and Mass Balance. After oral administration of a 100-mg dose of [^{14}C]milnacipran hydrochloride, the average peak plasma concentration among the four male healthy subjects without emesis was 239.6 ng/ml for unchanged milnacipran and 679.0 ng Eq of milnacipran/ml for ^{14}C radioactivity (Table 1), indicating that unchanged milnacipran contributed approximately 35% of the plasma radioactivity at the peak plasma concentration. The AUC_{0-t} of unchanged milnacipran was 2342.6 ng · h/ml and similarly contributed approximately 36% of the AUC_{0-t} of ^{14}C radioactivity (6446.3 ng Eq of milnacipran · h/ml). The results indicate that milnacipran metabolites were produced and observed in plasma after the oral administration of milnacipran hydrochloride. The average time to peak plasma concentration and half-life were 3.5 and 8.9 h, respectively, for unchanged milnacipran, compared with 4.3 and 7.7 h for ^{14}C radioactivity, respectively.

Approximately 97% of the radioactivity in the dose was recovered from the excreta (Table 2). On average, 93.3% of the dose (range, 91.3–94.3%) was excreted in urine, whereas 3.65% of the dose (range, 2.8–5.3%) was excreted in feces, indicating that urinary excretion was the principal route of elimination.

Metabolite Profile. A brief validation of the metabolite profile procedure was conducted to evaluate the sample processing recovery, chromatography resolution, HPLC column recovery, linearity of the analysis, and counting efficiency of the detector. The high recovery of radioactivity from plasma (average 81.0% of the plasma radioactivity)

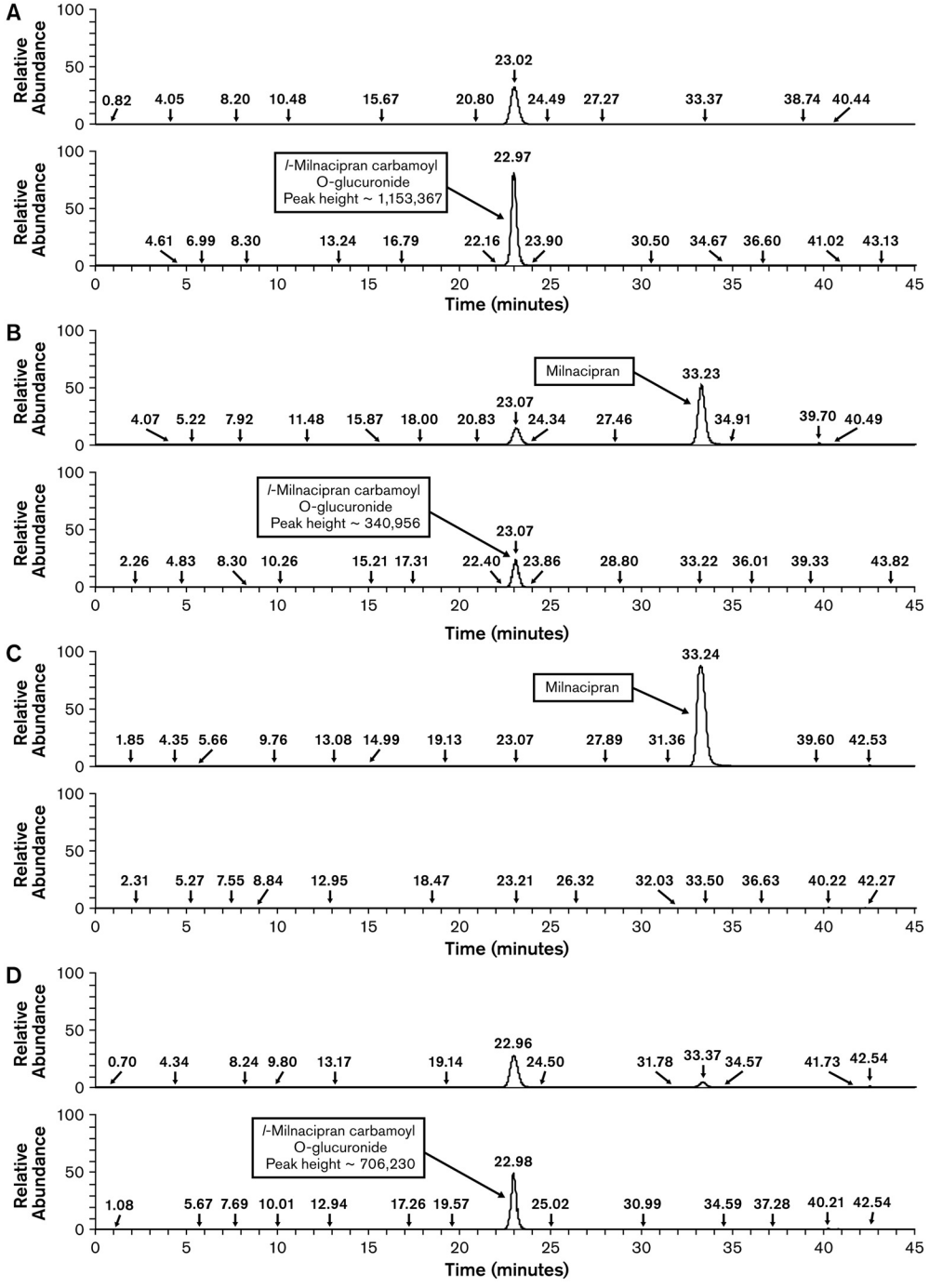

FIG. 6. The chromatograms from the analysis of the isolated peak 3 from the 0 to 4 h urine sample of subject 3 before hydrolysis (A), after treatment with 2 N hydrochloric acid at 70°C for 1 h (B), after treatment with Glusulase at 37°C for 1 h (C), and after treatment with Glusulase and the inhibitor, D-saccharic acid 1,4-lactone, at 37°C for 1 h (D). Milnacipran, *m/z* 247 → 230, retention time ~34 min; *l*-milnacipran carbamoyl *O*-glucuronide metabolite (peak 3), *m/z* 467 → 230, retention time ~23 min.

in sample processing, along with the high HPLC column recovery of radioactivity from the sample (average 99.1% of the sample radioactivity) in the HPLC analysis provided a thorough analysis of metabolites in the metabolite profile.

Plasma metabolite profiles. A total of five chromatographic peaks with measurable radioactivity were observed in the metabolite profile of plasma (Fig. 1A). Peak 3 was the major metabolite in plasma, with a maximum plasma concentration of approximately 234 ng Eq of milnacipran/ml (Table 3). The plasma concentration of peak 3 was similar to that of milnacipran (peak 5) for all plasma samples from 0.5 to 12 h. The plasma concentration of each remaining peak of the plasma metabolite profile was relatively low and did not exceed 25 ng Eq of milnacipran/ml. No other chromatographic peaks with significant radioactivity were observed in the plasma metabolite profile.

Urine metabolite profiles. Five distinct chromatographic peaks were also observed in the urine metabolite profiles (Fig. 1B; Table 4). The majority of milnacipran in the dose was excreted unchanged in urine (peak 5, average 55% of the dose), with peak 3 (average 17% of the dose) and peak 1 (average 7.7% of the dose) representing the major metabolites excreted in urine. Small amounts of peak 2 and peak 4 (neither exceeding 2.1% of the dose) were also excreted in urine. No other chromatographic peaks with significant radioactivity were observed in the urine metabolite profile. Chiral LC-SRM analysis of the 0 to 96 h urine pools showed that the renal excretion of *d*-milnacipran (31% of the dose) was slightly higher than that of *l*-milnacipran (24% of the dose) (Table 5).

Identification of Milnacipran and Its Metabolites. The chemical structures of unchanged milnacipran (peak 5) and milnacipran metabolites (peaks 1, 3, and 4) were identified using LC-MS/MS, LC-SRM, and LC-HRMS methods. Identification of the metabolite in peak 2 was not attempted because <2% of the dose was excreted as this peak. For LC-MS/MS and LC-SRM analyses, the chemical structure of a

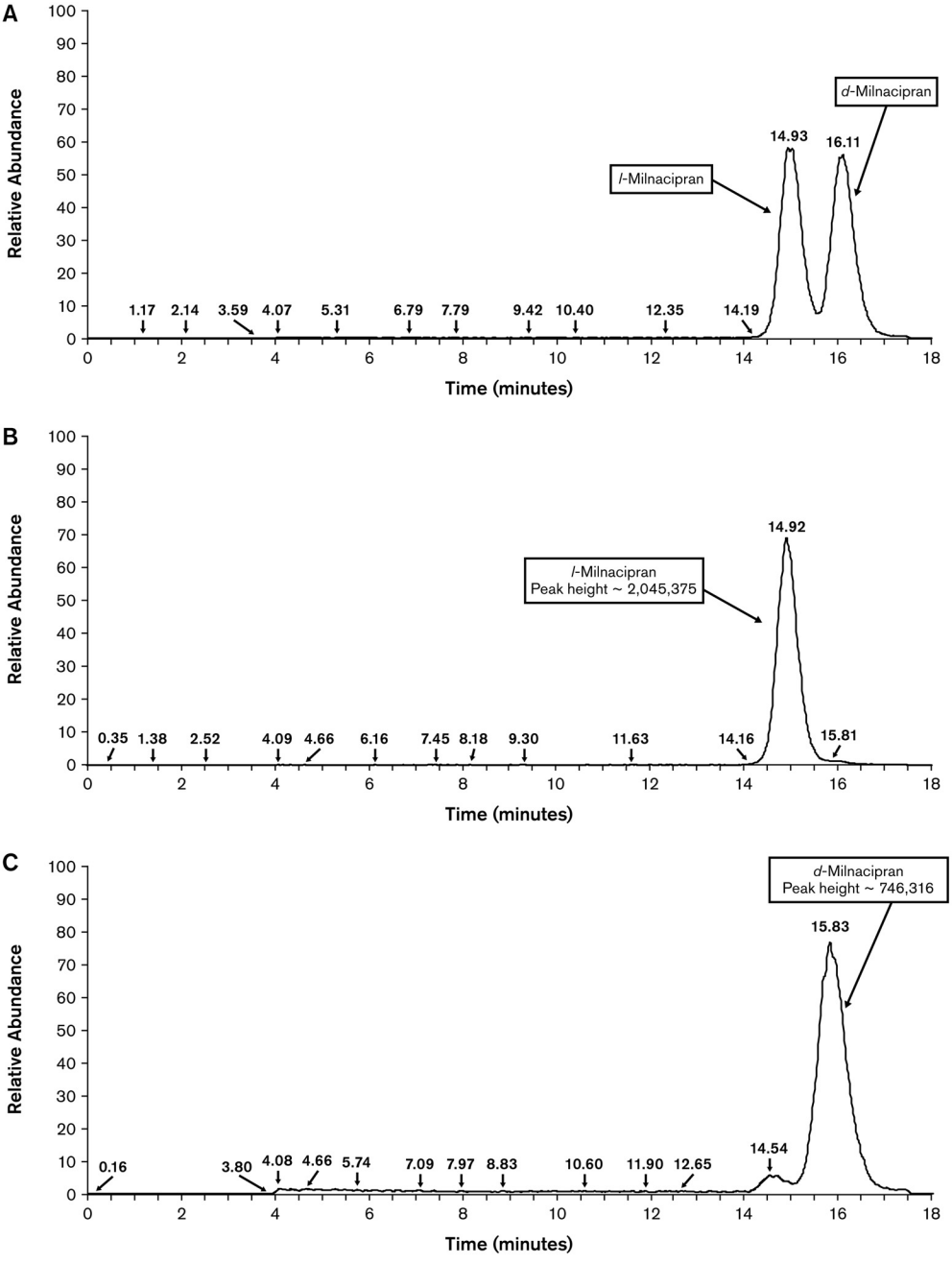

FIG. 7. The chiral LC-SRM analysis of racemic milnacipran standard (A), the *l*-milnacipran produced from hydrolysis of the isolated *l*-milnacipran carbamoyl *O*-glucuronide metabolite (peak 3) (B), and the *d*-milnacipran produced from hydrolysis of the isolated *d*-milnacipran carbamoyl *O*-glucuronide metabolite (peak 4) (C). Both metabolites were isolated from the 0 to 4 h urine sample of subject 1. *l*-Milnacipran, *m*/*z* 247 → 230, retention time ~15 min; *d*-milnacipran, *m*/*z* 247 → 230, retention time ~16 min.

metabolite was identified when retention time, protonated molecular ion, and mass spectrum (LC-MS/MS) or product ion (LC-SRM) were identical to those of the standard (biosynthetically or chemically synthesized). For the LC-HRMS analysis, the chemical structure was characterized when the protonated molecular ion of the metabolite was within ±15 ppm of the theoretical protonated molecular ion of the metabolite. Acid hydrolysis and enzyme hydrolysis were also conducted to confirm glucuronide metabolites in peaks 3 and 4 of the urine samples from two subjects.

Peak 1. The chemical structure of the metabolite eluted as peak 1 in the metabolite profile of urine was identified as *N*-desethyl milnacipran, which has a molecular weight of 218.29 and a monoisotopic molecular weight of 218.14. The retention time (11 min), protonated molecular ion (*m/z* 219) (Fig. 2A), and mass spectrum (Fig. 2B) of the metabolite observed in the LC-MS/MS analysis matched those of *N*-desethyl milnacipran standard (Fig. 3). A fragmentation scheme (Fig. 4) was proposed on the basis of the major fragments observed in the mass spectrum (*m/z* 202, *m/z* 174, and *m/z* 131) (Fig. 2B). It appeared that the amine function of the molecule was protonated to produce the protonated molecular ion (*m/z* 219). The fragment of *m/z* 202 was produced after a neutral loss of ammonia (NH_3, 17 Da) from the protonated molecular ion. The fragment of *m/z* 174 was produced after an additional neutral loss of ethene (C_2H_4, 28 Da) from the fragment of *m/z* 202. The protonated form of a lactam was the proposed structure for the fragment of *m/z* 174. The fragment of *m/z* 131 was produced by addition of a hydrogen molecule (2 Da) to the fragment generated by neutral losses of ammonia (NH_3, 17 Da) and carbon monoxide (CO, 28 Da) from the fragment of *m/z* 174. The carbonium ion of 1-methyl-2-phenyl-cyclopropane was the proposed structure for the fragment of *m/z* 131. The stability of the carbonium ion was probably provided by the electrons of the phenyl ring. The protonated molecular ion (*m/z* 219.1478) of the metabolite observed in the LC-HRMS analysis was accurate (6.3 ppm from theoretical) and supported the proposed structure. Peak 1 in the metabolite profile of plasma was also identified as the *N*-desethyl milnacipran metabolite using a similar procedure.

Peak 3. The chemical structure of the metabolite eluted as peak 3 in the metabolite profile of urine was identified as *l*-milnacipran carbamoyl *O*-glucuronide, which has a molecular weight of 466.48 and a monoisotopic molecular weight of 466.20. The retention time (22 min), protonated molecular ion (*m/z* 467) (Fig. 5A), and mass spectrum (Fig. 5B) of the metabolite observed in the LC-MS/MS analysis matched those of the *l*-milnacipran carbamoyl *O*-glucuronide biosynthetic standard (Fig. 3). Major fragments of *m/z* 291, *m/z* 247, and *m/z* 230 were observed in the mass spectrum (i.e., product ion spectrum) after the fragmentation of the protonated molecular ion. In addition, a minor fragment of *m/z* 449 was observed in the spectrum. It appeared that a nitrogen atom of the molecule was protonated to

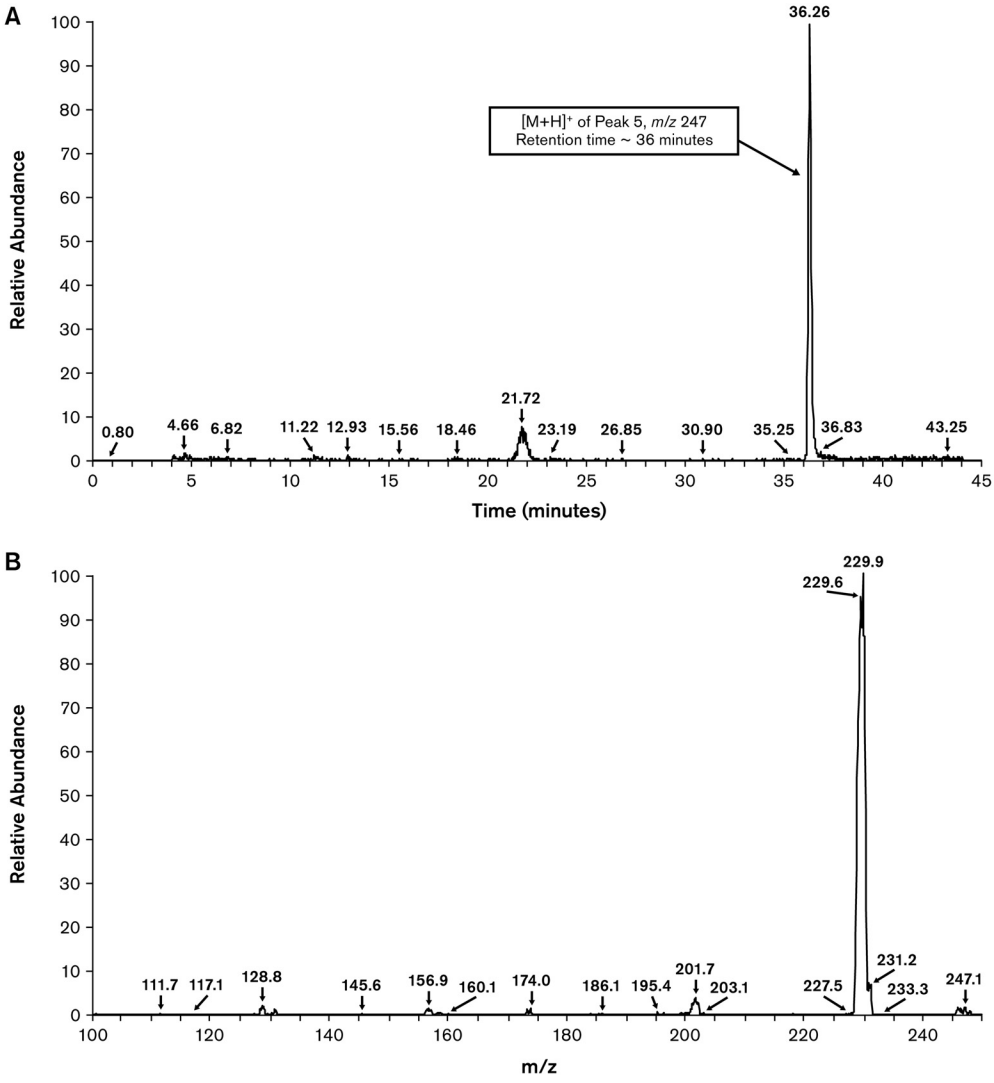

FIG. 8. LC-MS/MS analysis of unchanged milnacipran (peak 5, precursor ion = protonated molecular ion, *m/z* 247) in the 0 to 4 h urine sample of subject 1. A, protonated molecular ion of unchanged milnacipran. B, product ion spectrum produced by the protonated molecular ion of unchanged milnacipran.

produce the protonated molecular ion. The fragment of *m/z* 449 represented a neutral loss of a water molecule (H_2O, 18 Da) from the protonated molecular ion (*m/z* 467). The fragment of *m/z* 291 was produced by a neutral loss of dehydrated glucuronic acid moiety (176 Da) from the protonated molecular ion. The fragment of *m/z* 247 was produced after an additional neutral loss of carbon dioxide (44 Da) from the fragment of *m/z* 291. The fragment of *m/z* 230 was produced after a neutral loss of ammonia (17 Da) from the fragment of *m/z* 247. The protonated molecular ion (*m/z* 467.1974) of the metabolite observed in the LC-HRMS analysis was accurate (10.7 ppm from theoretical) and supported the proposed structure.

In addition, the hydrolysis of the urine metabolite in peak 3 to milnacipran (Fig. 6) by β-glucuronidase (selective hydrolysis) and acid (partial hydrolysis) was similar to the hydrolysis of the *l*-milnacipran carbamoyl *O*-glucuronide biosynthetic standard. The enzymatic hydrolysis was inhibited by D-saccharic acid 1,4-lactone, indicating that the metabolite was a β-glucuronide. It appeared that the aglycone produced from hydrolysis of the urine metabolite was a milnacipran carbamic acid, which underwent facile decarboxylation and appeared as milnacipran.

The *l*-isomer of milnacipran, *l*-milnacipran, was the enantiomer produced from the hydrolysis of isolated peak 3. After enzymatic hydrolysis of isolated peak 3 in urine samples from subject 1 and subject 3, *l*-milnacipran was the sole milnacipran enantiomer observed in the chiral analysis of the hydrolyzed product (Fig. 7B). These results indicate that *l*-milnacipran was metabolized and excreted in urine as *l*-milnacipran carbamoyl *O*-glucuronide metabolite (peak 3). Peak 3 in the metabolite profile of plasma was also identified as the *l*-milnacipran carbamoyl *O*-glucuronide metabolite using similar approaches with LC-SRM and chiral LC-SRM analyses.

Peak 4. The chemical structure of the metabolite eluted as peak 4 in the metabolite profile of urine was identified as *d*-milnacipran carbamoyl *O*-glucuronide. The retention time (24 min), protonated molecular ion (*m/z* 467), and mass spectrum of the metabolite observed in the LC-MS/MS analysis matched those of the *d*-milnacipran carbamoyl *O*-glucuronide biosynthetic standard (Fig. 3). Because the *d*- and *l*-milnacipran carbamoyl *O*-glucuronides are diastereomers, similar fragments (*m/z* 449, 291, 247, and 230) were observed in the mass spectra of both glucuronides. The protonated molecular ion (*m/z* 467.1968) of the peak 4 metabolite observed in the LC-HRMS analysis was accurate (12.0 ppm from theoretical) and also supported the proposed structure.

In addition, the hydrolysis of the urine metabolite in peak 4 to milnacipran by β-glucuronidase (selective hydrolysis) and acid (partial hydrolysis) was similar to the hydrolysis of the *d*-milnacipran carbamoyl *O*-glucuronide biosynthetic standard. The enzymatic hydrolysis was inhibited by D-saccharic acid 1,4-lactone, indicating that the metabolite was a β-glucuronide. It appeared that the aglycone produced from the hydrolysis of the urine metabolite was a milnacipran carbamic acid, which underwent facile decarboxylation and appeared as milnacipran.

The *d*-isomer of milnacipran, *d*-milnacipran, was the enantiomer produced from the hydrolysis of isolated peak 4. After the enzymatic hydrolysis of isolated peak 4 from subject 1 and subject 3, *d*-milnacipran was the sole milnacipran enantiomer observed by chiral analysis of the hydrolyzed product (Fig. 7C). Therefore, the results supported the fact that *d*-milnacipran was metabolized and excreted in urine as *d*-milnacipran carbamoyl *O*-glucuronide metabolite (peak 4). Peak 4 in the metabolite profile of plasma was also identified as the *d*-milnacipran carbamoyl *O*-glucuronide metabolite using a similar approach with LC-SRM analysis.

Peak 5. The chemical structure of the compound eluted as peak 5 in the metabolite profile of urine was identified as unchanged milnacipran, which has a molecular weight of 246.35 and a monoisotopic molecular weight of 246.17. The retention time (36 min), protonated molecular ion (*m/z* 247) (Fig. 8), and mass spectrum of the compound observed in the LC-MS/MS analysis matched those of the milnacipran standard (Fig. 3). The fragments of *m/z* 230, *m/z* 202, *m/z* 174, *m/z* 157, and *m/z* 129 observed in the mass spectrum after the fragmentation of the protonated molecular ion were similar to those observed in the fragmentation of the *N*-desethyl milnacipran metabolite (Fig. 4). It appeared that the amine function of the molecule was protonated to produce the protonated molecular ion (*m/z* 247). The fragment of *m/z* 230 was produced after a neutral loss of ammonia (NH_3, 17 Da) from the protonated molecular ion and was the predominant fragment observed in the mass spectrum. The fragment of *m/z* 202 was produced after a neutral loss of ethene (C_2H_4, 28 Da) from the fragment of *m/z* 230. The fragment of *m/z* 174 was produced after an additional neutral loss of ethene (C_2H_4, 28 Da) from the fragment of *m/z* 202. The protonated form of a lactam was the proposed structure for the fragment of *m/z* 174. The fragment of *m/z* 157 was produced after a neutral loss of ammonia (NH_3, 17 Da) from the fragment of *m/z* 174. The fragment of *m/z* 129 was produced after a neutral loss of carbon monoxide (CO, 28 Da) from the fragment of *m/z* 157. The protonated molecular ion (*m/z* 247.1778) of the compound observed in the LC-HRMS analysis was accurate (10.9 ppm from theoretical) and supported the proposed structure. Peak 5 in the metabolite profile of plasma was also identified as unchanged milnacipran using a similar procedure.

Discussion

After oral administration of a 100-mg dose of [^{14}C]milnacipran hydrochloride to healthy male volunteers, the radioactivity of almost the entire dose (approximately 93% of the dose) was excreted in urine within 96 h, signifying the excellent oral absorption of milnacipran. Renal excretion of unchanged milnacipran in humans appeared to be the major elimination route of milnacipran, accounting for approximately 55% of the dose. This study also found that the renal excretion of *d*-milnacipran (31% of the dose) was slightly higher than that of *l*-milnacipran (24% of the dose).

A major milnacipran metabolite, previously reported as milnacipran *N*-glucuronide (Puozzo et al., 1998), was ultimately identified in this study as *l*-milnacipran carbamoyl *O*-glucuronide. This major metabolite was excreted primarily in urine and accounted for approximately 17% of the dose. The *d*-milnacipran enantiomer was similarly converted to *d*-milnacipran carbamoyl *O*-glucuronide metabolite and excreted in urine, but it accounted for only 2% of the dose. This study also found that approximately 8% of the dose was excreted in urine as the *N*-desethyl milnacipran metabolite. No other metabolites with significant radioactivity were observed in urine. The biotransformation of milnacipran in humans is summarized in Fig. 9.

Because unchanged milnacipran accounted for only 36.3% of the AUC_{0-t} for plasma radioactivity (on average), it was expected that milnacipran metabolite(s) would be present in plasma after the oral administration of milnacipran hydrochloride. The milnacipran metabolites excreted in urine were also observed in plasma. The maximum concentration of the major plasma metabolite, the *l*-milnacipran carbamoyl *O*-glucuronide metabolite, was approximately 234 ng Eq of milnacipran/ml. In addition, the concentration of this metabolite was similar to that of milnacipran for all plasma samples collected during the 0.5 to 12 h after dosing. Therefore, the AUC of *l*-milnacipran carbamoyl *O*-glucuronide metabolite also accounted for approximately 36% of the AUC_{0-t} of plasma radioactivity. The plasma concentrations of the *N*-desethyl milnacipran and the *d*-milnacipran carbamoyl *O*-glucuronide metabolites were relatively low and did not

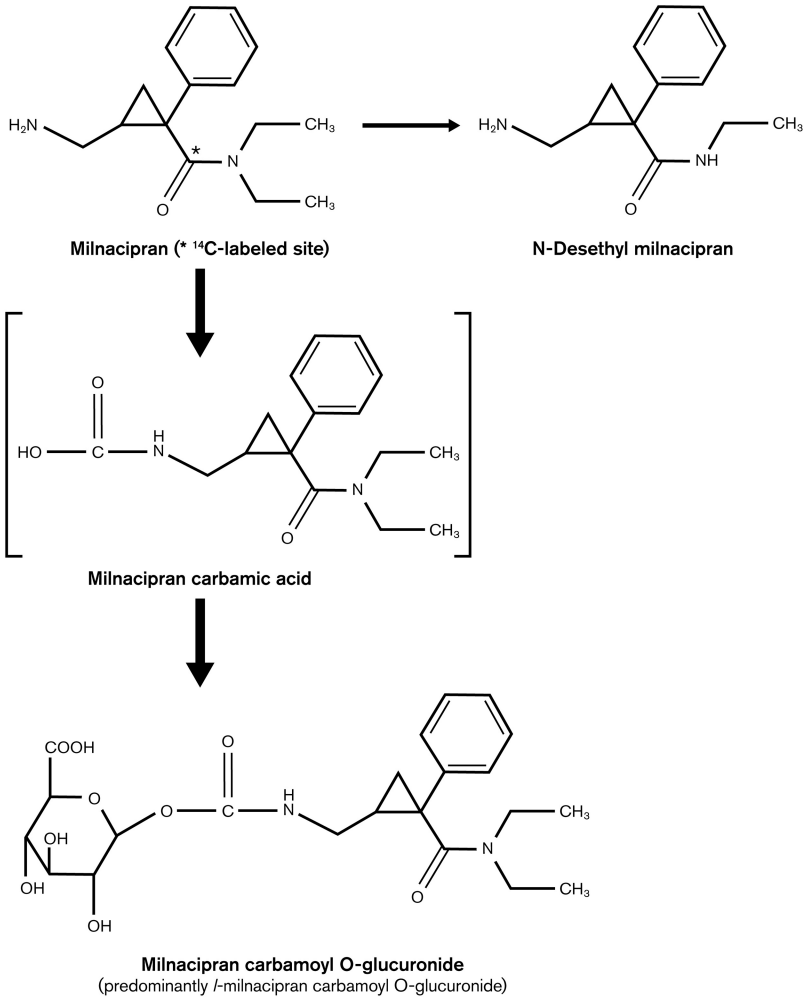

FIG. 9. Proposed metabolic transformation of milnacipran in humans.

exceed 25 ng Eq of milnacipran/ml. Thus, the AUCs of these two metabolites were not determined.

Similarly to other carbamoyl *O*-glucuronide metabolites (Tremaine et al., 1989; Delbressine et al., 1990; Schaefer, 1992; Schaefer et al., 1998), the milnacipran carbamoyl *O*-glucuronide metabolites were probably formed by a nonenzymatic reversible reaction of the primary amine function of milnacipran with carbon dioxide to form a milnacipran carbamic acid intermediate, which was subsequently conjugated to glucuronic acid. In this study, the milnacipran carbamoyl *O*-glucuronide metabolites were partially hydrolyzed by acid and selectively hydrolyzed by β-glucuronidase to its aglycone. The aglycone produced from hydrolysis of the glucuronide was a milnacipran carbamic acid, which underwent facile decarboxylation and appeared as milnacipran. Similar hydrolytic properties have been reported for the carbamoyl *O*-glucuronide metabolite of numerous compounds (Tremaine et al., 1989; Kwok et al., 1990; Schaefer, 1992).

In addition to the common neutral loss of 176 Da (i.e., dehydrated glucuronic acid moiety) from the protonated molecular ion of regular glucuronide metabolites, a unique neutral loss of 220 Da (i.e., the sum of dehydrated glucuronic acid moiety and carbon dioxide, 176 + 44 Da) from the protonated molecular ions of carbamoyl *O*-glucuronide metabolites has been frequently reported in the literature (Straub et al., 1988; Tremaine et al., 1989; Dow et al., 1994; Schaefer et al., 1998; Beconi et al., 2003). In this study, the fragments of *m/z* 247 and *m/z* 291 observed in the mass spectra of *d*- and *l*-milnacipran carbamoyl *O*-glucuronide metabolites support the occurrence of both types of neutral losses (220 and 176 Da) from the protonated molecular ions (*m/z* 467) of these metabolites. The mass spectra results also supported the chemical structure of milnacipran carbamoyl *O*-glucuronide metabolites.

A significant in-source (i.e., in the ionization source of the mass spectrometer) degradation of both *d*- and *l*-milnacipran carbamoyl *O*-glucuronide metabolites to milnacipran was observed when the biosynthetic standards, isolated peak 3, or isolated peak 4 were analyzed by LC-MS/MS and LC-SRM. Milnacipran generated in-source from milnacipran carbamoyl *O*-glucuronide metabolite should have the retention of milnacipran carbamoyl *O*-glucuronide metabolite. However, the retention time of milnacipran was much longer than that of milnacipran carbamoyl *O*-glucuronide metabolite in the analyses. Hence, the milnacipran generated in-source was easily distinguished from the milnacipran presented in the sample.

Milnacipran is not transformed to its *trans*-isomer in humans. The stereochemistry of milnacipran shows it to be a *cis*-isomer composed of a pair of enantiomers: *d*-milnacipran (1*S*, 2*R*) and *l*-milnacipran (1*R*, 2*S*). The *trans*-isomer of milnacipran is also a pair of enantiomers: the (1*R*, 2*R*) and (1*S*, 2*S*). To transform milnacipran to its *trans*-isomer would require changes at only one chiral center of milnacipran: (1*S*, 2*R*) to (1*R*, 2*R*) or (1*S*, 2*S*) and (1*R*, 2*S*) to (1*R*, 2*R*) or (1*S*, 2*S*). In this study, the HPLC method provided a good baseline resolution (Fig. 2) of the *trans*-isomer of milnacipran (retention time ~34 min) from milnacipran (retention time ~36 min). The *trans*-isomer of milnacipran was not observed in the metabolite profile of

plasma or urine by radioactivity analysis (Fig. 1, A and B, respectively). In addition, LC-MS/MS analysis of a urine sample (Fig. 8A) confirmed that milnacipran was not excreted in urine as its *trans*-isomer. The absence of milnacipran transformation to its *trans*-isomer would imply no chirality change at either chiral center of milnacipran. Furthermore, previous clinical studies of milnacipran have demonstrated that there is no interconversion between the *d*-milnacipran (1*S*, 2*R*) and *l*-milnacipran (1*R*, 2*S*) enantiomers (data on file, company study reports). The conversion of *d*-milnacipran to *l*-milnacipran, or vice versa, would require changes at both chiral centers: 1*S* to 1*R* and 2*R* to 2*S* (or vice versa). Therefore, the absence of the milnacipran transformation to its *trans*-isomer in this study (no change in either chiral center) strengthens the results of previous clinical studies (no change in both chiral centers).

Previously, the metabolism of milnacipran was studied after oral administration of [^{14}C]milnacipran hydrochloride to mice (100 mg/kg), rats (100 mg/kg), and monkeys (60 mg/kg) (data on file, company study reports). After the oral administration, approximately 40% of the dose (monkeys) to 63% of the dose (rodents) was excreted in urine as unchanged milnacipran. Less than 2% of the dose was excreted as the milnacipran carbamoyl *O*-glucuronide metabolite in mice (1.0% of the dose), rats (0.1% of the dose), and monkeys (1.6% of the dose). Similar amounts of *d*- and *l*-milnacipran carbamoyl *O*-glucuronide metabolites were excreted by each animal species, and both glucuronide metabolites were observed in plasma of all three animal species. In addition, milnacipran was transformed to *N*-desethyl milnacipran metabolite in the animals, with the *N*-desethyl milnacipran metabolite being the major metabolite produced in rats and monkeys. The animal plasma concentrations of *N*-desethyl milnacipran metabolite and *d*-milnacipran carbamoyl *O*-glucuronide metabolite were higher than those observed in humans (100-mg oral dose). Moreover, the plasma concentration of *l*-milnacipran carbamoyl *O*-glucuronide metabolite found in monkeys was similar to that observed in humans, but lower plasma concentrations of this metabolite were found in mice and rats.

Overall, the metabolism study of milnacipran hydrochloride was conducted safely in humans. Other than the common side effect of emesis observed in two healthy subjects, the 100-mg oral dose of [^{14}C]milnacipran hydrochloride was well tolerated by the remaining healthy subjects. In addition to measuring all major plasma metabolites of milnacipran in this study, the excretion of milnacipran and its major metabolites was measured. We hope that the results of this comprehensive study of milnacipran metabolism in humans will help scientists and physicians better understand the therapeutic usage of milnacipran hydrochloride.

Acknowledgments

We thank Melanie Ronsheim and Thomas Chou for their assistance with the analyses of the study. In addition, we thank Larry Cheng for his guidance during the study, as well as Dr. Morgan Hill and Mildred Bahn at Prescott Medical Communications Group (Chicago, IL) for editorial and medical writing assistance.

Authorship Contributions

Participated in research design: Li, Wangsa, and Ho.
Conducted experiments: Li and Chin.
Performed data analysis: Li, Chin, Wangsa, and Ho.
Wrote or contributed to the writing of the manuscript: Li, Wangsa, and Ho.

References

Beconi MG, Mao A, Liu DQ, Kochansky C, Pereira T, Raab C, Pearson P, and Lee Chiu SH (2003) Metabolism and pharmacokinetics of a dipeptidyl peptidase IV inhibitor in rats, dogs, and monkeys with selective carbamoyl glucuronidation of the primary amine in dogs. *Drug Metab Dispos* **31:**1269–1277.
Delbressine LP, Funke CW, van Tilborg M, and Kaspersen FM (1990) On the formation of carbamate glucuronides. *Xenobiotica* **20:**133–134.
Dow J, Piriou F, Wolf E, Dulery BD, and Haegele KD (1994) Novel carbamate metabolites of mofegiline, a primary amine monoamine oxidase B inhibitor, in dogs and humans. *Drug Metab Dispos* **22:**738–749.
Forest Laboratories, Inc. (2009) Savella (milnacipran hydrochloride) full prescribing information. Forest Laboratories, Inc., New York.
Gibaldi M and Perrier D (1975) Pharmacokinetics, 2nd ed., *Drugs and the Pharmaceutical Sciences*, vol 1, Marcel Dekker Inc., New York.
Kwok DW, Pillai G, Vaughan R, Axelson JE, and McErlane KM (1990) Preparative high-performance liquid chromatography and preparative thin-layer chromatography isolation of tocainide carbamoyl-*O*-β-D-glucuronide: structural characterization by gas chromatography-mass spectrometry and fast atom bombardment-mass spectrometry. *J Pharm Sci* **79:**857–861.
Puech A, Montgomery SA, Prost JF, Solles A, and Briley M (1997) Milnacipran, a new serotonin and noradrenaline reuptake inhibitor: an overview of its antidepressant activity and clinical tolerability. *Int Clin Psychopharmacol* **12:**99–108.
Puozzo C, Albin H, Vinçon G, Deprez D, Raymond JM, and Amouretti M (1998) Pharmacokinetics of milnacipran in liver impairment. *Eur J Drug Metab Pharmacokinet* **23:**273–279.
Puozzo C and Leonard BE (1996) Pharmacokinetics of milnacipran in comparison with other antidepressants. *Int J Clin Psychopharmacol* **11 (Suppl 4):**S15–S27.
Puozzo C, Panconi A, and Depez D (2002) Pharmacology and pharmacokinetics of milnacipran. *Int Clin Psychopharmacol* **17 (Suppl 1):**S25–S35.
Schaefer WH (1992) Formation of a carbamoyl glucuronide conjugate of carvedilol in vitro using dog and rat liver microsomes. *Drug Metab Dispos* **20:**130–133.
Schaefer WH, Politowski J, Hwang B, Dixon F Jr, Goalwin A, Gutzait L, Anderson K, DeBrosse C, Bean M, and Rhodes GR (1998) Metabolism of carvedilol in dogs, rats, and mice. *Drug Metab Dispos* **26:**958–969.
Straub K, Davis M, and Hwang B (1988) Benzazepine metabolism revisited. Evidence for the formation of novel amine conjugates. *Drug Metab Dispos* **16:**359–366.
Tremaine LM, Stroh JG, and Ronfeld RA (1989) Characterization of a carbamic acid ester glucuronide of the secondary amine sertraline. *Drug Metab Dispos* **17:**58–63.

Address correspondence to: Dr. John Ho, Forest Research Institute, 220 Sea Lane, Farmingdale, NY 11735. E-mail: john.ho@frx.com